Nucleation rate and number of precipitates in V and Nb-microalloyed steels

Sebastián F. Medina[1,a*] and Manuel Gómez[1,b]

[1]National Centre for Metallurgical Research (CENIM-CSIC), Av. Gregorio del Amo 8, 28040-Madrid (Spain)

[a]smedina@cenim.csic.es, [b]mgomez@cenim.csic.es

Keywords: microalloyed steels, precipitate, nucleus size, nucleation rate

Abstract. Recrystallization-precipitation-time-temperature (RPTT) diagrams were experimentally determined for two microalloyed steels with V and Nb, respectively, at a strain of 0.35 and a strain rate of 3.63 s^{-1}. From the RPTT diagrams, and applying the classic theory of nucleation, the nucleation rate was calculated for both steels. In order to determine the mentioned magnitudes, several parameters were calculated, such as: the Zeldovich factor (Z), the energy of formation of the nucleus (ΔG), the driving force for precipitation (ΔGv), the critical radius for nucleation (Rc), and the dislocation density at the start of precipitation (ρ), among others. The calculated data has made it possible to clarify the shape of precipitation start and finish curves and to plot the nucleation rate as a function of temperature. The number of precipitates was calculated by integration of the nucleation rate expression. In this way, substantial differences were established between the two types of microalloyed steels, including the final size of the V(C, N) and Nb(C, N) precipitates.

Introduction

Microalloyed steels are strengthened mainly by the dispersion of fine precipitate particles and their effect on the inhibition of grain growth, the progress of static recrystallization and the movement of dislocations [1]. These steels are usually soaked at high temperatures where the roughing deformation is carried out. Nb, V, and to a lesser extent Ti are the most commonly used microalloying elements. Upon cooling they combine with C and/or N to form carbide, nitride and/or carbonitride precipitates. The deformation of austenite increases the dislocation density and causes a significant acceleration of the nucleation, growth and coarsening of precipitates [2-4].

The hot deformation of austenite sets the stage for two competing processes, namely static recrystallization and strain-induced precipitation. The interaction of these two phenomena has been widely studied by a number of researchers, who have considered different variables such as the steel composition, strain, strain rate, austenite grain size and deformation temperature, among others.

Precipitation is assumed to take place in two stages. In the first stage the precipitates nucleate and grow, and in the second stage, when nucleation ceases, the precipitates enter a regime of growth and coarsening [5].

The coarsening of precipitates, leading to the growth of larger precipitates at the expense of smaller precipitates, cannot occur if diffusion is dominated by volume diffusion. These observations can only be explained by considering the effect of accelerated solute diffusion along the dislocations [6].

In order to understand the mechanisms of precipitation during hot working, the nucleation rate and number of precipitates have been calculated in two microalloyed steels with V and Nb as microalloying elements, respectively, applying the classic theory of nucleation [6-8].

Materials and experimental procedure

The steels were manufactured by electroslag remelting in a laboratory unit capable of producing 30 kg ingots. Their compositions are shown in Table 1. The two steels include different microalloying elements such as V (steel V) and Nb (steel N), respectively. Given that the nitrides, carbides or

carbonitrides of Nb are less soluble in austenite than those of V, the limit imposed on C and N contents has been that the solubility temperature should not exceed 1300ºC.

Table 1. Chemical composition (mass %) and transformation critical temperature (A_{r3}, 0.2 K/s).

Steel	C	Si	Mn	Al	X_i	N	A_{r3} , °C
V	0.33	0.22	1.24	0.011	V=0.076	0.0146	716
N	0.11	0.24	1.23	0.002	Nb=0.041	0.0112	786

Torsion specimens were prepared with a gauge length of 50 mm and 6 mm diameter. The reheating temperature prior to torsion deformation was different depending on whether the steel was microalloyed with V or with Nb (Table 1), as the solubility temperature of the precipitates depends on their nature and on the precipitate-forming element content. For steel V, the reheating temperature was 1200ºC, which is sufficient to dissolve vanadium nitrides and carbides. In the case of steel N, the reheating temperature was 1230ºC, above the solubility temperature of niobium carbonitrides [9].

To ensure that the testing temperatures corresponded to the austenitic phase, critical transformation temperatures were measured by dilatometry at a cooling rate of 0.2ºC/s (**Table 1**). The magnitudes of torsion (torque, no. of revolutions) and the equivalent magnitudes (stress, strain) have been related according to Von Mises criterion [10]. The torsion specimens were tested at a strain of 0.35 and a constant strain rate of 3.63 s^{-1} (=1000 rev/min). The strain of 0.35 in no case exceeded the peak strain necessary for dynamic recrystallization to commence in any of the steels [11].

Results and discussion

RPTT diagrams. Recrystallized fraction curves can be used to plot recrystallization-precipitation-time-temperature (RPTT) diagrams [12,13]. The points that define the start and end of the plateau were taken to plot the induced precipitation start (P_s) and finish (P_f) curves, respectively. The temperatures and times corresponding to different recrystallized fractions were also deduced from recrystallized fraction curves. In this way we have drawn the RPTT diagrams corresponding to steels V and N, respectively (Figs. 1 and 2). Note that the recrystallized fraction does not vary between the precipitation start (P_s) and finish (P_f) curves and is represented by a horizontal line. Once the P_f curve is reached, the lines of each recrystallized fraction descend, meaning that as the temperature drops, more time is necessary to obtain a certain recrystallized fraction after straining.

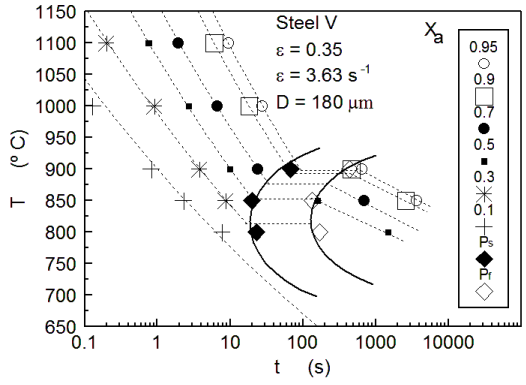

Fig. 1. RPTT diagram for steel Nb.

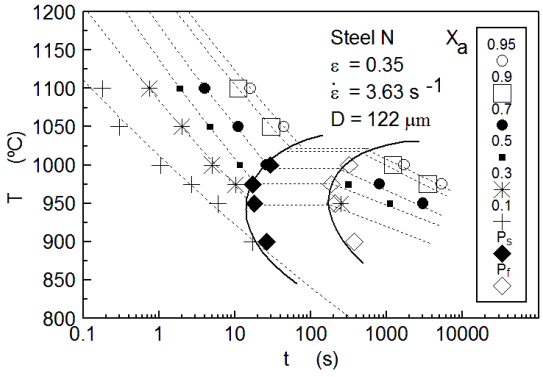

Fig. 2. RPTT diagram for steel V.

With regard to the recrystallization-precipitation interaction, it is seen that at the nose of the P_s curve, where the incubation time of the precipitates (t_N) is minimal, the recrystallized volume fraction is approximately 50%. The most important magnitudes that can be deduced from an RPTT diagram, which are also indispensable for the perfect configuration of the diagram, are the aforementioned minimum incubation time (t_N), the minimum precipitation end time (t'_N), the curve nose temperature (T_N) and finally the precipitation duration time (t'_N-t_N). T_N is approximately

825ºC for steel V and 950ºC for steel N. This difference is due to the greater solubility of V in austenite, and thus the occurrence of precipitation at a lower temperature in steel V than in steel N.

At the moment when precipitation starts, whatever the temperature (P_s curve), it is assumed that the precipitated fraction corresponds to a value of 5% ($t_{0.05}$). In the same way, when the P_f curve is reached, the precipitated volume is close to 95% ($t_{0.95}$). Once the P_f curve has been reached, recrystallization starts to progress again due to fact that the pinning forces exerted by the precipitates are lower than the driving forces for recrystallization.

Precipitation nucleation rate. The nucleation rate is obtained from the classic theory of nucleation modified by Zeldovich, Kampamann and Wagner [8,14] as:

$$\frac{dN}{dt} = N_0 Z\beta' \exp\left(-\frac{\Delta G}{kT}\right)\exp\left(-\frac{\tau}{t}\right) \tag{1}$$

where, N_0 represents the number of available sites for heterogeneous nucleation, Z is de Zeldovich non-equilibrium factor, k is the Boltzman constant, β' is the rate at which the atoms are being added to the critical nucleus or atomic impingement rate, T is the absolute temperature, τ is the incubation time and ΔG is the Gibbs energy of formation of a critical spherical nucleus of radius R_c.

On the other hand, the terminus $\exp(-\tau/t)$ indicates the progress of the nucleation rate, but most authors do not take into account as the nucleation period is very short. Neglecting the strain energy term, the Gibbs energy for the formation of a spherical nucleus of carbonitride from the elements in solution (V,Nb) is classically expressed as the sum of a volume and an interface term [6,15-17]:

$$\Delta G(J) = -\frac{4}{3}\pi R_c^3 \Delta G_v + 4\pi\gamma R_c^2 = \frac{16\pi\gamma^3}{3\Delta G_v^2} \tag{2}$$

where γ is the surface energy of the precipitate (0.5 Jm^{-2}) and ΔG_v is the driving force for precipitation given by [6]:

$$\Delta G_v\left(Jm^{-3}\right) = -\frac{R_g T}{V_m}\ln\left(\frac{C_x C_y}{C_x^e C_y^e}\right) \tag{3}$$

where C_x and C_y are the instantaneous concentrations of V or Nb and N or/and C, respectively, C_x^e and C_y^e are the equilibrium concentrations at the deformation temperature, V_m is the molar volume of precipitate species, R_g is the universal gas constant and T is the deformation temperature. $N_0=0.5\Delta\rho^{1.5}$ is the number of nodes in the dislocation network, $\Delta\rho=(\Delta\sigma/0.2\mu b)^2$ is the variation in the density of dislocations associated with the recrystallization front movement in the deformed zone at the start of precipitation [5], $\Delta\sigma$ is the difference between the flow stress and yield stress at the deformation temperature, b is the Burgers vector and μ is the shear modulus.

The atomic impingement rate is given as [6]:

$$\beta'\left(s^{-1}\right) = \frac{4\pi R_c^2 D C_x}{a^4} \tag{4}$$

where D is the bulk diffusivity of solute atoms (Nb,V) in the austenite, a is the lattice parameter of the precipitate and C_x is the initial concentration of solute.

The Zeldovich factor Z takes into account that the nucleus is destabilized by thermal excitation compared to the inactivated state and is given as [18]:

$$Z = \frac{V_{at}^p}{2\pi R_c^2}\sqrt{\frac{\gamma}{kT}} \tag{5}$$

According to Turkdogan [19], the supersaturation ratio defined by $K_s = \frac{C_x C_y}{C_x^e C_y^e}$ will be:

Nb-Steels:

$$K_s = \frac{[Nb][C]^{0.7}[N]^{0.2}}{\left[10^{4.12-\frac{9450}{T}}\right]} \quad (6)$$

V-Steels:

$$K_s = \frac{[V][N]}{\left[10^{2.86-\frac{7700}{T}}\right]} \quad (7)$$

It has been considered that Nb forms carbonitrides and V forms nitrides with the stoichiometry used by Turkdogan. The values used for different physical parameters are listed in Table 2.

If the term exp(-τ/t) in equation (1) is dismissed, then the nucleation rate is a function only of temperature. A graphic representation of dN/dt versus temperature is shown in Fig. 3. In the calculations it has not been taken into account whether the microstructure is partly recrystallized, as can be seen in the RPTT diagrams. As will be noted in the following chapter, the precipitation time for the 5% precipitated volume ($t_{0.05}$) deduced from Figs. 1 and 2 is much higher than the nucleation time (τ) by more than one order of magnitude, and this means that at this moment the recrystallized fraction is negligible whatever the temperature. Therefore, the dislocation density has been calculated using the model reported by Medina and Hernández [11] which facilitates the calculation of the flow stress.

On the other hand, the integration of equation (1) would give the number of precipitates per unit of volume (N). Fig. 4 shows the value of N for two temperatures that correspond to the minimum incubation times in Figs. 1 and 2, respectively. For steel V the temperature corresponding to the nose of the P_s curve was 825ºC, and for steel N it was approximately 950ºC. Although the value of N increases constantly, this is only apparent because growth and coarsening, which would cause the value of N to decrease, passing through a maximum [6], have not been taken into account.

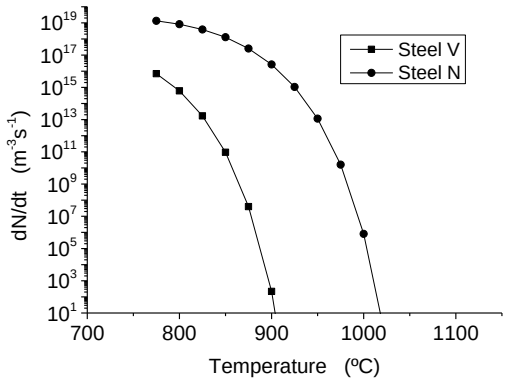

Fig. 3. Nucleation rate vs. temperature.

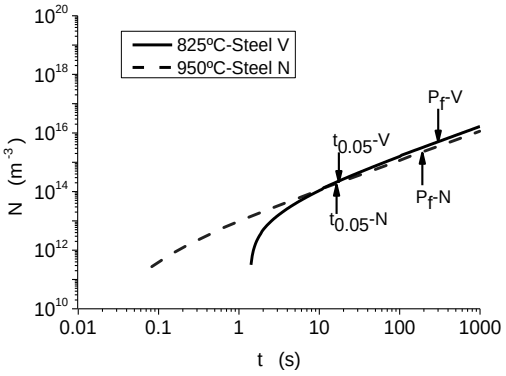

Fig. 4. Precipitate number vs. time.

Nucleation critical time (τ) and critical radius of precipitate. In equation (1) the incubation time (τ) is given as follows [20]:

$$\tau = \frac{1}{2\beta' Z^2} \quad (8)$$

The values calculated for τ in the two steels are shown as a function of the temperature (Fig. 5). These values are much smaller than the experimental $t_{0.05}$ values shown in Figs. 1 and 2, which

correspond to the precipitation start curve P_s. On the other hand, if the energy for pipe diffusion were taken into account in equation (4) instead of the energy for bulk diffusion, the values of τ would be two orders of magnitude lower, i.e. nucleation would be instantaneous and would take place in an infinitesimally short time. For their part, the minimum nucleation times achieved correspond to temperatures above those of the nose of the P_s curve in Figs. 1 and 2. Thus there is some disagreement between the calculated and the experimental values.

The critical radius for nucleation is determined from the driving force and is given as:

$$R_c = -\frac{2\gamma}{\Delta G_v} \tag{9}$$

R_c was calculated for the two steels as a function of temperature (Fig. 6). The calculated critical radii are smaller than those measured in V-microalloyed steels, whose average size at the nose of the curve is approximately 6 nm [21].

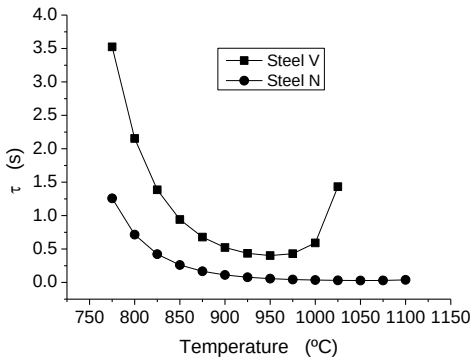

Fig. 5. Nucleation critical time vs. temperature.

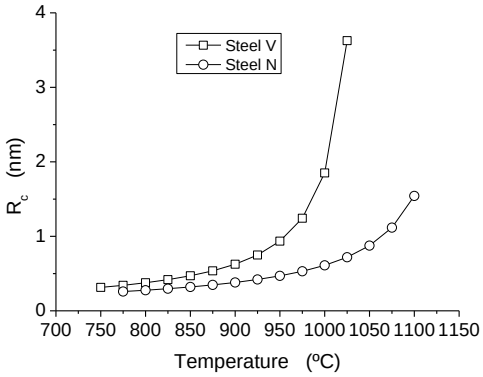

Fig. 6. Precipitate critical radius vs. temperature.

Thus it is shown that the experimental $t_{0.05}$ time (P_s curve) in Figs. 1 and 2 does not exactly correspond to the start of nucleation, but that the first nuclei of precipitates form at much shorter times, in such a way that between the moment when the first precipitates form and the moment of $t_{0.05}$ corresponding to the nose of the P_s curve, when the precipitates were analyzed, considerable growth of the precipitates has occurred [21].

The R_c values are higher for steel V than for steel N because the driving force for precipitation, ΔG_v, is lower in absolute terms for the latter. Moreover, the incubation time τ is longer for steel V because the Zeldovich factor is one order of magnitude lower for this steel.

Table 2. Parameters used for calculations.

Parameter	Symbol	Value	Reference
Molar volume (NbCN)	V_m (m^3/mol)	$1.305x10^{-5}$	23
Molar volume (VN)	V_m (m^3/mol)	$1.052x10^{-5}$	23
Atomic volume (NbCN)	V_{at} (m^3)	$2.1678x10^{-29}$	calculated
Atomic volume (VN)	V_{at} (m^3)	$1.6468x10^{-29}$	calculated
Burgers vector	b (m)	$2.59x10^{-10}$	5
Shear modulus	μ (MPa)	$4x10^4$	22,23
Interfacial energy	γ (Jm^{-2})	0.5	6,16
Lattice parameter (VN)	a (nm)	0.4161	25
Lattice parameter (NbCN)	a (nm)	0.4445	6
V diffusivity in austenite	D (m^2s^{-1})	$0.28x10^{-4}exp(-264000/RT)$	24
Nb diffusivity in austenite	D (m^2s^{-1})	$1.4x10^{-4}exp(-270000/RT)$	6

Conclusions

The calculated nucleation time (τ) is much shorter than the $t_{0.05}$ time determined experimentally for the two studied steels. Furthermore, considerable growth of the precipitates has taken place between these two moments.

The nucleation rate as a function of temperature is lower for steel V than for steel N. This is due to the greater solubility of V in austenite compared to Nb.

Both the nucleation rate and the number of precipitates per unit of volume are approximately the same in both steels when the calculations are carried out at the nose temperature of the experimental P_s curve.

The incubation time and the critical radius for nucleation are greater for steel V than for steel N.

References

[1] K. Xu, B.G. Thomas, R. O'Malley, Metall. Mater. Trans. A. 42 (2011) 524-539.
[2] C.M. Sellars: Mater. Sci Technol. 6 (1990) 1072-1081.
[3] E. J. Palmiere, C.I. Garcia, A.J. DeArdo, Metall. Mater. Trans. A 25 (1994) 277-286.
[4] W.J. Liu, Metall. Mater. Trans. A 26 (1995) 1641-1657.
[5] B. Dutta, E, Valdes, C.M. Sellars: Acta Metall. Mater. 40 (1992) 653-662.
[6] B. Dutta, E.J. Palmiere, C.M. Sellars, Acta Mater. 49 (2001) 785-794.
[7] K.C. Russel, Adv. Colloid. Interface Sci. 13 (1980) 205-318.
[8] R. Kampmann, R. Wagner: Mater. Sci. Tech. A Comprenhensive Treatment, ed. R.W. Cahn, P. Hassen and E.J. Krammer, VCH Verlagsgesselschaft mbH, Weinheim, 1991, vol. 5, p. 213.
[9] E.T. Turkdogan: Iron Steelmaker 3 (1989) 61-75.
[10] A. Faessel: Rev. Métall,. Cah.Inf.Tech. 33 (1976) 875-892.
[11] S.F. Medina and C.A. Hernández: Acta Mater. 44 (1996) 155-163.
[12] M. Gómez, S. F. Medina, A. Quispe, P. Valles: ISIJ Int. 42 (2002) 423-431.
[13] S.F. Medina, A. Quispe, M. Gómez: Mater. Sci. Technol. 19 (2003) 99-108.
[14] M. Perez, M. Dumont, D. Acevedo-Reyes: Acta Mater. 56 (2008) 2119-2132.
[15] N. Fujita, H.K.D.H. Bhadeshia: Mater. Sci. Tecnol. 17 (2001) 403-408.
[16] P. Maugis, M. Gouné: Acta Mater. 53 (2005) 3359-3367.
[17] W.P. Sun, M. Militzer, D.Q. Bai, J.J. Jonas: Acta metal. Mater. 41 (1993) 3595-3604.
[18] B. Dutta, E. Valdes, C.M. Sellars: Acta Metall. Mater. 40(1992) 653-662.
[19] F. Perrard, A. Deschamps, P. Maugis: Acta Mater. 55 (2007) 1255-1266.
[20] E.T. Turkdogan: Iron Steelmaker 16 [1989] 61-75.
[21] M. Perez, D. Acevedo-Reyes, T. Courtois, E. Epicier, P. Maugis: Phil. Mag. Lett. 87 (2007) 645-656.
[22] S.F. Medina**,** L. Rancel, M. Gómez, R. Ishak, M. de Sanctis: ISIJ Int. 48 (2008) 1603-1608.
[23] T. Gladman: The physical metallurgy of microalloyed steels, The Institute of Materials, London,1997.
[24] S. Vervynckt, K. Verbeken, P. Thibaux, Y. Houbaert: Mater. Sci. Eng. A. 528 (2011) 5519-5528.
[25] H. Oikawa: Tetsu-to-hagane 68 (1982) 1489-1497.
[26] T. Furuhara, J. Yamaguchi, N. Sugita, G. Miyamoto, T. Maki: ISIJ Int. 43 (2003) 1630-1639.